



ELSEVIER

15 April 2002

Optics Communications 205 (2002) 207–213

OPTICS  
COMMUNICATIONS

www.elsevier.com/locate/optcom

# Simplified cavity designs for efficient and compact femtosecond Cr:LiSAF lasers

B. Agate<sup>a,\*</sup>, B. Stormont<sup>b</sup>, A.J. Kemp<sup>a</sup>, C.T.A. Brown<sup>a,b</sup>, U. Keller<sup>c</sup>, W. Sibbett<sup>a,b</sup>

<sup>a</sup> *J.F. Allen Physics Research Laboratories, School of Physics & Astronomy, University of St. Andrews, St. Andrews, KY16 9SS Scotland, UK*

<sup>b</sup> *Ultrafast Photonics Collaboration, School of Physics & Astronomy, University of St. Andrews, St. Andrews, KY16 9SS Scotland, UK*

<sup>c</sup> *Physics Department, Institute of Quantum Electronics, Swiss Federal Institute of Technology (ETH), Zurich, Switzerland*

Received 20 December 2001; accepted 5 March 2002

## Abstract

We describe efficient, compact femtosecond Cr:LiSAF lasers with a reduced component count that combine greater simplicity with improved performance. We observe transform-limited pulses as short as 136 fs centered on 859 nm at a 470 MHz repetition rate. 20 mW of average output power has been achieved for less than 100 mW of incident diode-laser pump power – an optical-to-optical conversion efficiency of over 20%. We have demonstrated an entirely portable, self-contained, battery-powered version of this laser on a  $22 \times 28$  cm<sup>2</sup> breadboard, with an electrical-to-optical efficiency of almost 4%. Using four pump laser diodes, we have also achieved operational regimes providing either gigahertz repetition rates or kilowatt peak powers. © 2002 Elsevier Science B.V. All rights reserved.

## 1. Introduction

One of the objectives of ultrashort pulse laser research is to develop simple, inexpensive and robust femtosecond lasers that open up applications previously inaccessible to bulky, lab-bound systems. A promising route to simplifying femtosecond lasers has involved the use of low-threshold cavity designs, and optical pumping with narrow-stripe, single spatial mode laser diodes [1,2]. With compact pump stage designs, improved use of available diode pump power, and new methods of

prismless dispersion compensation [3,4] to reduce the component count, a considerable reduction in laser footprint is now possible, while increasing operational efficiencies and maintaining satisfactory levels of performance [5].

The most important breakthrough in size reduction has come through innovative approaches to dispersion compensation. With the conventional intracavity prism-pair, the required separation is often impractically large, and therefore recent demonstrations of single-prism [6] and prismless dispersion-compensation schemes [7,8] are of particular interest. Given that presently available chirped mirrors have losses that are too high for their incorporation in low-pump-threshold femtosecond lasers, alternative, low-loss dis-

\* Corresponding author. Fax: +44-1334-463-104.  
E-mail address: mba@st-andrews.ac.uk (B. Agate).

persion-compensating elements such as the Gires–Tournois interferometer (GTI) mirror [7,9] are being considered. To facilitate robust modelocking at low intracavity powers, modelocking is readily initiated with the well-established semiconductor saturable absorber mirror (SESAM) [10]. This modelocking element has a low insertion loss and creates an entirely self-starting mechanism for modelocking.

In this Letter we report several simplified, efficient and reduced-scale femtosecond Cr:LiSAF laser cavity configurations, which take advantage of a compact and integrated approach to dispersion compensation. Whereas typical modelocked titanium–sapphire lasers exhibit electrical–optical conversion efficiencies of 0.004–0.04% [11], we describe an ultracompact, entirely portable femtosecond laser source with an impressive electrical-to-optical efficiency of nearly 4%. We believe this to represent the highest reported efficiency for any femtosecond laser.

## 2. Low-threshold cavity design

A key factor in the development of these compact and efficient lasers is minimization of the lasing threshold, and a number of design criteria must be met in order to reduce the required pump power. Firstly, the intracavity losses are minimized through the use of a SESAM which has been designed to be low-loss, and by reducing the component count, where methods of prismless dispersion compensation are undoubtedly of particular importance. The SESAM is a broadband, low-finesse A-FPSA (antiresonant Fabry–Perot saturable absorber), identical to that described in [12]. In this Letter, we describe a dispersion compensation scheme which is fully integrated within the cavity design and allows for very compact laser resonators. This cavity configuration which requires no additional intracavity element beyond the SESAM modelocking element, laser crystal, output coupler and dichroic high-reflecting fold mirrors is discussed in detail in Section 4.

In using a Brewster-angled Cr:LiSAF laser crystal having both high pump absorption and large emission cross-section, upper-state lifetime ( $\sigma\tau$ )

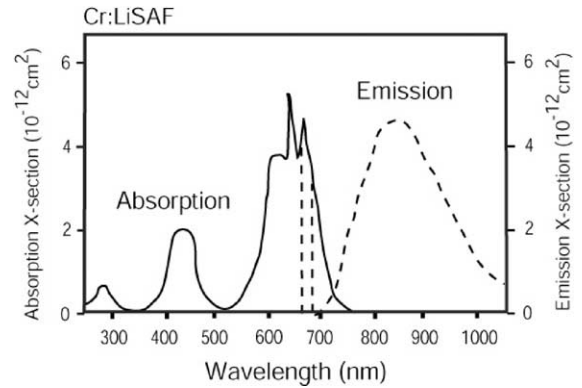


Fig. 1. The absorption and emission spectra of Cr:LiSAF [17]. The two central dashed lines show the wavelengths of the commercially available AlGaInP pump diodes, at 660 and 685 nm.

product, low operational thresholds are also ensured [13]. The Cr:LiSAF gain crystal not only satisfies the necessary spectroscopic requirements, including an appropriately broad absorption band around 650 nm and a broadband emission spectrum of almost 400 nm (Fig. 1) which can support very short pulses of  $\sim 10$  fs [14], but its thermal conductivity, although poor in comparison to titanium–sapphire ( $k_{\text{Cr:LiSAF}} = 3.1 \text{ W m}^{-1} \text{ K}^{-1}$ ;  $k_{\text{Ti:Sapphire}} = 25$ ) means that at respectable pump powers ( $\sim 100$  mW), active crystal cooling is not required. The significant advantage that Cr:LiSAF holds over titanium–sapphire, in respect of the  $\sigma\tau$  products already mentioned, is clear from  $\sigma\tau_{\text{Ti:Sapphire}} = 1.3 \times 10^{-24} \text{ cm}^2 \text{ s}$  and  $\sigma\tau_{\text{Cr:LiSAF}} = 3.4 \times 10^{-24} \text{ cm}^2 \text{ s}$ .

The use of a Brewster-angled laser crystal requires an astigmatically compensating, highly asymmetric Z-cavity design [1] (Fig. 2). The asymmetry of this laser cavity allows us to achieve tight foci in the laser crystal ( $w_{\text{pump}} \sim 11 \mu\text{m}$ ;  $w_{\text{laser}} \sim 20 \mu\text{m}$ ) and on the SESAM ( $w_{\text{laser}} \sim 40 \mu\text{m}$ ), which contribute to low cw and modelocking thresholds, respectively [2].

Because the absorption peak of Cr:LiSAF lies at 650 nm, the direct pumping of the crystal becomes immediately accessible with readily available GaInP/AlGaInP red diodes, whereas blue-green laser diode technology is as yet insufficiently developed for diode-pumping of Ti:Sapphire. Devices from Hitachi (HL6503MG) and Mitsubishi (ML1013R) exist with output powers

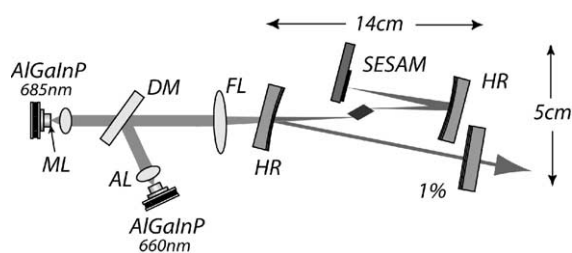


Fig. 2. Schematic of a diode-pumped, compact femtosecond laser cavity with wavelength-combining coupling optics and integrated dispersion compensation. (ML: microlens; AL: aspheric lens; DM: dichroic mirror; FL: focusing lens; HR: high reflector; 1%: output coupler.)

of 50 and 60 mW at 660 and 685 nm, respectively (Fig. 1). These inexpensive, narrow-stripe laser diodes have much better beam quality and lower astigmatism than their broad-stripe counterparts, and their diffraction-limited output allows for an improved mode overlap within the gain medium. Therefore, as well as reducing the size of the cavity footprint, we have been able to design more compact pump stages by simplifying the coupling optics.

The standard method of coupling together a pair of pump diodes is that of polarization coupling. In this technique, an s-polarized diode, rotated 90° in polarization by a half-wave plate (HWP), is combined with a p-polarized diode in a polarizing beam-combining cube. However, this is not the most efficient use of available pump power as losses are incurred both in the beam-combining cube and significantly (~10%) by the s-polarization at the incident surface of the Brewster-angled crystal.

The availability of commercial AlGaInP red pump diodes at two different wavelengths (660 and 685 nm) near the peak of the Cr:LiSAF absorption has allowed us to use wavelength-combining as a more efficient technique of diode-coupling. Significantly, wavelength-combining (Fig. 2) simplifies the optics and reduces the component count of the pump-stage mechanics. A simple off-the-shelf dichroic mirror (Chroma Technology Corp.), coated for high-transmission at 685 nm and high-reflection at 660 nm, is used as the coupling optic in place of a HWP and combining cube.

Circularization of the elliptical diode beams is achieved with the insertion of a microlens inside the diode can such that excellent mode overlap can be achieved in the laser without resorting to anamorphic prism pairs or cylindrical lens combinations. In our system, where the anisotropic Cr:LiSAF crystal is Brewster-angled, we achieve a 15% increase in absorbed pump power compared to the more conventional polarization coupling.

### 3. Compact, femtosecond Cr:LiSAF laser

In this configuration, the laser crystal is pumped with two wavelength-combined AlGaInP diodes (660 and 685 nm). The resonator includes only a 3 mm (5.5 at.-%-doped) Cr:LiSAF laser crystal, two dichroic high-reflectors, an SESAM modelocking element and an output coupler, as illustrated in Fig. 2. We observe the generation of transform-limited pulses of 136 fs duration centered at 859 nm (Fig. 3) and at a repetition rate of 470 MHz. Average output powers of up to

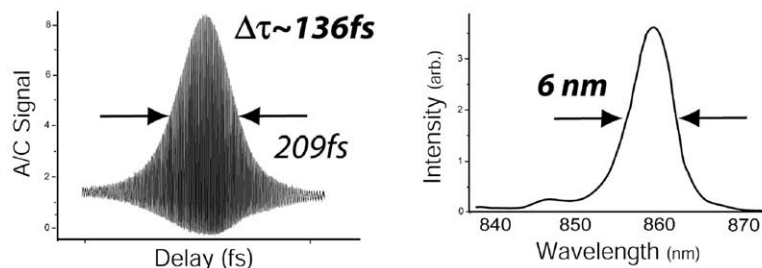


Fig. 3. Autocorrelation trace of 136 fs pulses and measured spectrum, with spectral bandwidth of 6 nm centered at 859 nm, achieved with the laser shown in Fig. 2.

20 mW have been achieved for  $\sim 95$  mW of incident pump power, giving an optical-optical efficiency of 21%. With the spectral bandwidth of  $\sim 6$  nm this implied a time-bandwidth product of 0.33. The amplitude stability of the laser output was observed to be very stable with a measured fluctuation of less than 1% for periods in excess of 1 h. These measurements were made on a laser that was not enclosed and located in a lab that was not temperature-controlled. In a more enclosed and controlled local environment we would expect the amplitude fluctuations of this laser to be extremely small.

#### 4. Dispersion compensation

The dispersion compensation in this laser was provided by the dichroic folding mirrors (high-reflectors (HR) in Fig. 2), which exhibit negative group delay dispersion (GDD) in the spectral region of laser operation. Although this was not a specified property of the coating, this identified feature facilitates a more integrated and compact methodology for dispersion compensation and this has some similarity with the SESAM-based method reported by Kopf et al. [4]. For our particular mirror coating this has provided adequate negative GDD across sufficient bandwidth to support transform-limited femtosecond pulses such that it was not necessary to tune the laser to a specific wavelength in order to exploit the negative GDD characteristic.

We performed a dispersion measurement on the HR mirrors using white-light interferometry [15], and found that the key feature of the optical coating was a periodic drop in group delay (GD) that extended over an acceptably broad wavelength range near the Cr:LiSAF lasing wavelength, as illustrated in Fig. 4. From the GDD versus wavelength characteristic, it can be seen that the dispersion curve of the HR mirrors is similar to that of a GTI type of mirror [9] which has dispersion-compensating features. We believe that fabrication effects in the manufacture of the HR mirror structure have led to the observed GD spikes. Initial investigations suggest that the observed GD profile is consistent with a series of high-finesse GTI-type structures.

The advantage that these HR mirrors hold over conventional GTI mirrors, however, is that they offer a high transmission at the pump wavelength, and can therefore be used as input couplers. Although initial analysis of the HR mirrors was unable to provide accurate numerical data, it is clear from experimentation that the amount of generated negative GDD is significant. [Detailed analysis of the HR mirrors is currently underway to accurately ascertain the magnitude of the GDD they introduce at the lasing wavelength.]

#### 5. Ultra-compact femtosecond laser source

To further reduce the footprint of the laser, we have constructed a version of the laser using small-

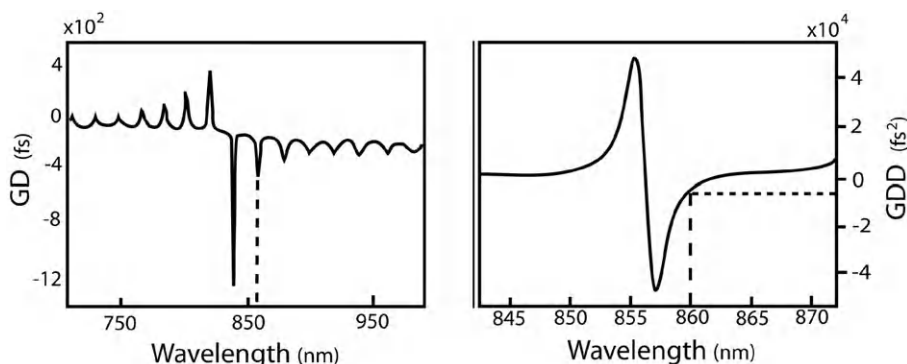


Fig. 4. Group delay (GD) and group delay dispersion (GDD) versus wavelength for the HR mirrors. The position of the central lasing wavelength is shown by a dashed line.

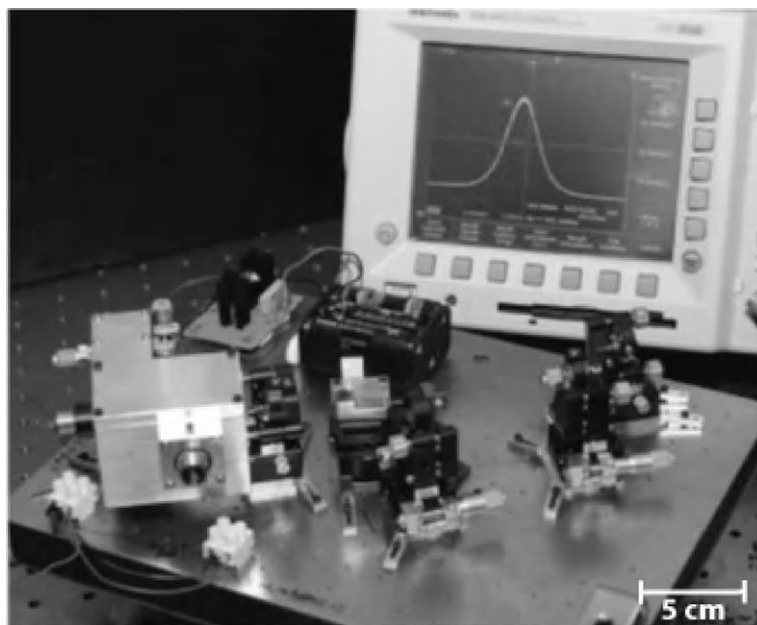


Fig. 5. Photograph of a highly efficient, self-contained, compact femtosecond laser. The pump stage, power source and laser cavity all sit on a  $22 \times 28 \text{ cm}^2$  breadboard.

scale optomechanical components. This miniature femtosecond laser, shown in Fig. 5, is powered by just six penlight (AA) batteries (the electrical drive power is less than 1 W) and is therefore entirely portable. These batteries enable modelocked operation to be achieved for more than 12 h. The entire laser system, including the pump stage, power source and drive electronics, fits on a  $22 \times 28 \text{ cm}^2$  breadboard, and operates with an electrical–optical efficiency of almost 4%, which is to the authors knowledge the highest reported efficiency for any femtosecond laser. Initial results have demonstrated pulses of 130 fs, at an average output power of 14 mW and a time-bandwidth product of 0.42. We expect the time-bandwidth product to be reduced when the dispersion compensation is fully optimized.

## 6. Kilowatt peak-power and gigahertz repetition-rate versions

We have also demonstrated the flexibility of this compact, low-threshold laser system by pumping it

with two pairs of diode lasers (total pump power  $\sim 180 \text{ mW}$ ) to achieve kilowatt pulse peak powers (Fig. 6) as well as gigahertz repetition rates [16]. Specifically, we have generated 122 fs pulses at average powers of 35 mW – an optical–optical efficiency of 20%. This corresponded to peak powers of 1.2 kW and a time-bandwidth product of  $\sim 0.3$ . The gigahertz pulse repetition-rate system, which is to our knowledge the highest reported repetition rate for a directly diode-pumped, non-harmonically modelocked bulk femtosecond laser, demonstrated transform-limited 146 fs pulses at an average output power of 3 mW and a repetition rate of 1.002 GHz. With such a high pulse repetition rate, the pulse energy is lower and so an output coupler of 0.07% transmission was required to ensure the saturation of the SESAM for stable modelocking.

Given that kilowatt peak powers can be generated, this system now represents a possible compact source for use in broad continuum generation from photonic crystal fibers. Techniques in nonlinear optics such as harmonic generation also become more attractive, where such a system could

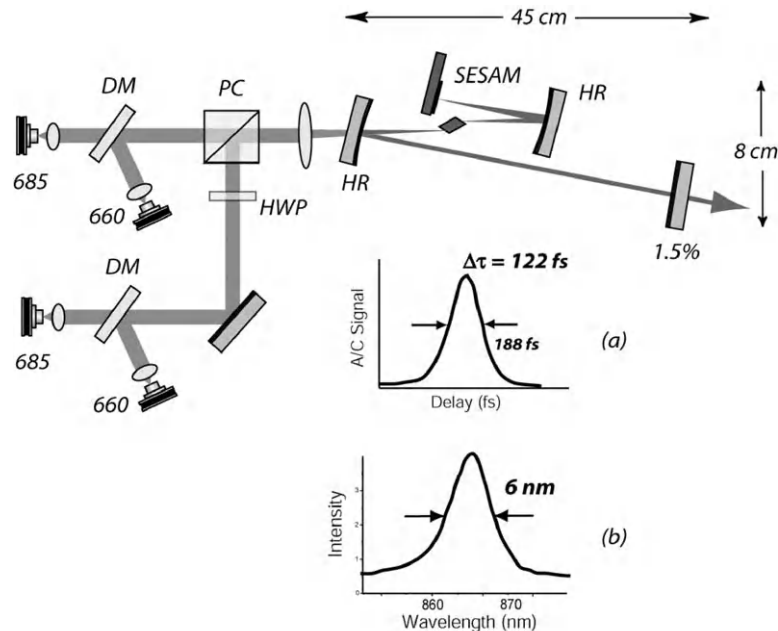


Fig. 6. Schematic of the kilowatt peak-power cavity, pumped with two pairs of AlGaInP diodes. (DM: dichroic mirror; HWP: half-wave plate; PC: polarisation beam splitter cube; HR: high reflector; 1.5%: output coupler.) Inset: (a) autocorrelation trace of 122 fs pulses from this laser; (b) measured spectrum, with spectral bandwidth of 6 nm centered at 865 nm.

be a very attractive and efficient source of ultra-short pulses in the blue spectral region.

Both the kilowatt and gigahertz configurations utilize very simple cavity geometries and again demonstrate the effectiveness of a compact and integrated approach to dispersion compensation. Indeed, because of the short cavity length (150 mm) and low round-trip losses, the gigahertz cavity would be very difficult to implement using less integrated methods of dispersion compensation.

## 7. Conclusions

In conclusion, we have shown that it is now entirely practical to design efficient, reduced-scale, femtosecond lasers having sufficiently low mode-locking thresholds to allow direct pumping with cheap, narrow-stripe AlGaInP laser diodes. An integrated approach to dispersion compensation reduces the component count and so further enhances the physical compactness and cost-effec-

tiveness of these lasers. The ability to generate stable femtosecond pulses either with kilowatt peak powers or at gigahertz repetition rates proves that these designs afford an attractive degree of flexibility and thus have the potential to open up applications that had been previously inaccessible to their lab-bound larger predecessors.

## Acknowledgements

The authors wish to acknowledge financial support from the UK Engineering and Physical Sciences Research Council (EPSRC).

## References

- [1] G.J. Valentine, J.-M. Hopkins, P. Loza-Alvarez, G.T. Kennedy, W. Sibbett, D. Burns, A. Valster, *Opt. Lett.* 22 (1997) 1639.
- [2] J.-M. Hopkins, G.J. Valentine, W. Sibbett, J.A. der Au, F. Morier-Genoud, U. Keller, A. Valster, *Opt. Commun.* 154 (1998) 54.

- [3] I. Sorokina, T.E. Sorokin, E. Wintner, A. Cassanho, T. Jensen, R. Szipocs, *Opt. Lett.* 22 (1994) 1716.
- [4] D. Kopf, G. Zhang, R. Fluck, M. Moser, U. Keller, *Opt. Lett.* 21 (1996) 486.
- [5] B. Agate, A.J. Kemp, J.-M. Hopkins, D. Burns, U. Keller, W. Sibbett, in: *Conference on Lasers and Electro-Optics (CLEO)*, Paper CMF2, Baltimore, MD, 2001.
- [6] D. Kopf, G.J. Spuhler, K.J. Weingarten, U. Keller, *Appl. Opt.* 35 (1996) 912.
- [7] A. Robertson, U. Ernst, R. Knappe, R. Wallenstein, V. Scheuer, T. Tschudi, D. Burns, M.D. Dawson, A.I. Ferguson, *Opt. Commun.* 163 (1999) 38.
- [8] R. Szipocs, A. Kohazi-Kis, S. Lako, P. Apai, A.P. Kovacs, G. DeBell, L. Mott, A.W. Louderback, A.V. Tikhonravov, M.K. Trubetskov, *Appl. Phys. B* 70 (2000) S51.
- [9] I. Gires, P. Tournois, *C. R. Acad. Sci.* 258 (1964) 6112.
- [10] U. Keller, K.J. Weingarten, F.X. Kartner, D. Kopf, B. Braun, I.D. Jung, R. Fluck, C. Honninger, N. Matuschek, J.A. der Au, *IEEE J. Selected Topics Quantum Electron.* 2 (1996) 435.
- [11] S. Tsuda, W.H. Knox, S.T. Cundiff, *Appl. Phys. Lett.* 69 (1996) 1538.
- [12] D. Kopf, A. Prasad, G. Zhang, M. Moser, U. Keller, *Opt. Lett.* 22 (1997) 621.
- [13] A.J. Alfrey, *IEEE J. Quantum Electron.* 25 (1989) 760.
- [14] S. Uemura, K. Torizuka, *Opt. Lett.* 24 (1999) 780.
- [15] K. Naganuma, K. Mogi, H. Yamada, *Opt. Lett.* 9 (1990) 393.
- [16] A.J. Kemp, B. Stormont, B. Agate, C.T.A. Brown, U. Keller, W. Sibbett, *Electron. Lett.* 37 (2001) 1457.
- [17] S.A. Payne, L.L. Chase, L.K. Smith, W.L. Kway, H.W. Newkirk, *J. Appl. Phys.* 66 (1989) 1051.